Role of nitrogen split interstitial defects in the magnetic properties of Cu-doped GaN

Y. Liu, Z. Gai, M. Weinert, and L. Li

Phys. Rev. B **85**, 075207 — Published 13 February 2012

DOI: 10.1103/PhysRevB.85.075207

The role of N split interstitial defect in the magnetic properties of Cu-doped GaN

Y. Liu[1], Z. Gai[2], M. Weinert[1], and L. Li[1]*

[1]Department of Physics, University of Wisconsin, Milwaukee, WI 53211, USA

[2] CNMS, Oak Ridge National Laboratory, Oak Ridge, TN, USA

Abstract:

Cu-doped GaN thin films are grown by plasma-assisted molecular beam epitaxy. With nitrogen plasma only, films phase segregate into GaN and Cu-rich alloys. In contrast, when nitrogen-hydrogen plasma is used, the films are single-phased $Ga_{1-x}Cu_xN$, with x as high as 0.04. Contrary to earlier studies, however, these films are not ferromagnetic, but rather paramagnetic in nature. First-principles calculations indicate that although each substitutional Cu_{Ga} exhibits a moment of 1 μ_B/Cu, it can be suppressed by neighboring intrinsic defects such as N split-interstitials.

PACS: 75.50.Pp, 71.15.Mb, 81.15.Hi, 68.55.A-,61.72.jj, 64.75.Qr

*lianli@uwm.edu

I. Introduction

Diluted magnetic semiconductors based on III-V and III-N doped with transition metal (TM) elements are of particular interest for applications in spintronics[1-7]. The challenge is to synthesize homogeneous materials doped with high enough concentrations of the TM ions to achieve Curie temperature above 300 K[8]. Recently, Cu-doped GaN thin films and nanowires have attracted considerable attention[9-19]. The incorporation of Cu naturally evades the question of dopant-phases being the source of the ferromagnetic ordering observed, since neither metallic Cu nor any possible phases in the Cu-N and Cu-Ga systems are ferromagnetic. Earlier density-functional-theory calculations for Cu-doped GaN indicated robust ferromagnetism with 100% spin polarization of the conduction carriers and a Curie temperature above 300 K[9]. In addition, a large total magnetization of 2.0 μ_B/Cu was also predicted. More recent calculations, however, showed only weak ferromagnetic behavior with the magnetic moment sensitive to Cu-Cu separation and defects such as N vacancy[10]. Experimental investigations have been carried out for Cu-doped GaN nanowires[13], Cu-implanted GaN films[14-16], chemical vapor deposited[17] and molecular beam epitaxy (MBE) grown Cu-doped GaN films[18,19]. All studies have shown room-temperature ferromagnetism. Nevertheless, the magnetic properties are found to be sensitive to Cu doping levels as well as the method of growth and Cu incorporation. For Cu-implanted samples, annealing is necessary to obtain ferromagnetic behavior and defects such as N vacancy are found to strongly affect the observed magnetism[16]. For MBE grown Cu-doped GaN, phase segregation has been a prevalent issue[18,19].

In this work, we report on the suppression of phase segregation during MBE growth of Cu-doped GaN by using nitrogen-hydrogen plasma. Our results indicate that single-phased $Ga_{1-x}Cu_xN$ can be grown with x as high as 0.04. Contrary to the earlier studies[18,19], however, these

films are not ferromagnetic, but rather paramagnetic in nature. These results are explained by first-principles calculations that indicate that each substitutional Cu_{Ga} exhibits a moment of $1\mu_B$/Cu. However, the moment is suppressed when Cu_{Ga} is adjacent to intrinsic defects such as a N split-interstitial. These results indicate that if the potential of Cu-doped GaN as a diluted magnetic semiconductor is to become a reality, the impact of intrinsic defects on its electronic and magnetic properties must be fully accounted for.

II. Methods

The substrates are 6H-SiC(0001) nitrogen-doped with a dopant concentration of ~10^{18} cm^{-2} (Cree Research Inc.), cleaned by resistively heating to 850-950 °C *in situ*. A flux of Si atoms was directed onto the heated SiC surface from an evaporator that consists of a resistively heated small Si wafer (3x5 mm^2) positioned 2 cm away. This process produced a (3x3) reconstruction, as observed by reflection high-energy electron diffraction and scanning tunneling microscopy[20]. A GaN buffer layer ~100 nm thick was first grown at 550-600 °C at a rate of 40 nm/hr. Gallium was provided by an effusion cell kept at 1000-1020 °C, while nitrogen reactive species were produced by the electron cyclotron resonance plasma source at 30 W with an N_2 flow rate of 3.0 sccm, and a total pressure of ~1x10^{-4} Torr during deposition. The growth of Cu-doped GaN was carried out at 500-550 ^oC with Cu supplied by an electron beam evaporator, during which the Ga cell temperature was reduced to 950 ^oC and the N_2 flow rate kept the same at 3.0 sccm. Two types of plasma conditions were employed: with N_2 gas only; or with a mixture of N_2/H_2 gas where 1-3 sccm of H_2 was also added to generate hydrogen reactive species. As a result, the growth conditions were changed from Ga-rich during buffer layer growth to N-rich during Cu doping[21]. The results presented below are for Cu-doped GaN films of 100-150 nm thick.

III. Results and Discussions

Presented in Figs. 1(a) & (b) are scanning electron microscopy (SEM) images of films grown using N_2 and N_2/H_2 plasma, respectively. With the N_2 plasma (Fig. 1(a)), the film surface is characterized by two distinct domains, boxed "A" and "B", where type *A* are randomly distributed strips and clusters, and *B* is featureless. The population and size of type *A* features increase with increasing Cu concentrations, suggesting that they are Cu enriched phases. In contrast, when N_2/H_2 plasma is used (Fig. 1(b)), a featureless surface is obtained over a wide range of Cu concentrations as described below.

Representative energy dispersive spectroscopy (EDS) spectra taken at regions marked *A*-*C* in Figs. 1(a) & (b) are shown in Fig. 1(c). For films grown with N_2 plasma, while 3.7% Cu is detected at the featureless domains, much higher concentrations up to 17% are found in the strips and clusters. The Cu content was calculated using the $K_{\alpha 1}$ peak ratios between Cu and Ga, taking into account of their sensitivity factors of 1.003 and 0.924, respectively. Since the x-ray has an escape length larger than one millimeter, the concentration obtained is a good indication of Cu in the bulk of the film. These observations clearly indicate that the Cu-doped GaN films grown with N_2 plasma has segregated into two phases, GaCuN and a Cu-rich secondary phase, consistent with earlier studies[18,19]. In contrast, with the presence of hydrogen in the plasma, single-phased $Ga_{1-x}Cu_xN$ can be grown with x as high as 0.04 within the resolution of SEM and EDS. This result is similar to our earlier work on the Mn doping of GaN using N_2/H_2 plasma, where a homogeneous Mn concentration as high as 6% was achieved[21]. The suppression of phase segregation has been attributed to the change of the growth mode from Ga-rich to N-rich, as well as reduced Mn mobility in the presence of hydrogen[22].

To further evaluate the effects of adding hydrogen to the plasma during growth, x-ray diffraction (XRD) is used to assess the crystallinity and structure of the films. Figure 2 presents XRD patterns for a Cu-doped GaN film (4% Cu) 100 nm thick. The insert is a close-up view of the peaks around the GaN (0002) peak at 34.61°. Note that the shoulder at 34.71° is caused by the $K_{\alpha 2}$ emission of the x-ray source. Based on analysis of rocking curves, the full-width-at-half-maximum (FWHM) is found to be 648 arcsec, indicating high film quality. Nevertheless, compared to the FWHM of ~600 arcsec for the phase segregated films, and 150 arcsec for the GaN buffer layers, both of which are grown under Ga-rich conditions (where the GaN buffer is also grown at a higher temperature), the crystallinity of these films is degraded. This is consistent with the general observation that the highest quality GaN films are grown under Ga-rich conditions as a result of the surfactant effect of the Ga adlayers[23,24].

Magnetic properties of these homogeneous $Ga_{1-x}Cu_xN$ films are characterized by a Quantum Design magnetic property measurement system. For comparison, the magnetic measurements of a pair of 100 nm $Ga_{1-x}Cu_xN$ films (x=0 and x=0.04) are shown in Fig. 3. The magnetic field dependence of the magnetization (M) are measured at 4.2 and 298 K up to 7 T (Fig. 3(a)), where no hysteresis and no variation from the Brillouin function are observed[25], indicating that the samples are not ferromagnetic, but rather paramagnetic in nature. The temperature (T) dependence of the magnetization of GaN films with and without Cu dopants (black and blue) taken in a 500 Oe magnetic field applied parallel to the film surface are presented in Fig. 3(b). Both curves show rapid and monotonic decrease at low temperatures, and excellent fits to Curie's law M=C·H/T, where *C* is the Curie constant and *H* the applied field. The estimated impurity concentration from the Curie constant is about $1x10^{-4}$ atomic ratio to Si in the undoped samples, the same order as the paramagnetic impurities typically found in SiC substrates,

suggesting that the paramagnetic signal mostly originates from impurities in the SiC substrate. Similarly, the Curie constant for the Cu-doped GaN sample is extracted, which is about four times larger than that of undoped GaN film. It is likely that a similar impurity/defect-induced mechanism is at play for the Cu-doped GaN films, however, with a higher density due to additional defects introduced during Cu doping.

These results are in clear contrast to earlier studies, where room temperature ferromagnetic ordering was reported in MBE grown Cu-doped GaN[18,19]. This may be related to several differences in the growth and structure of the films. First, Cu-rich islands are present on the Cu-doped GaN films in the earlier studies, which can contribute to the ferromagnetism observed. A recent study has shown that nanoparticles of a variety of inorganic materials can exhibit room-temperature ferromagnetism, even though their bulk counterparts are intrinsically non-magnetic[26]. For example, nanoparticles of GaN 15-20 nm in size have shown to be ferromagnetic, while larger particles (>150 nm) exhibit diamagnetic behavior. The observed ferromagnetic ordering in the smaller GaN nanoparticles have been attributed to the formation of Ga or N vacancies near the surface of these materials[26].

On another hand, although we have produced single-phased GaCuN films using N_2/H_2 plasma, the likely presence of intrinsic defects must also be taken into account, particularly N split-interstitial defects that are commonly found in GaN films prepared by plasma-assisted MBE under N-rich conditions[27,28], and GaN nanowires grown by the catalytic vapor-phase transport method[29]. To address role of these defects on the electronic and magnetic properties of Cu-doped GaN, first-principles spin-polarized generalized gradient approximation (GGA) electronic structure calculations were done using the Full-potential Linearized Augmented Plane Wave (FLAPW) method[30]. The calculations used 3×3×2 supercells (nominally 72 atoms), and included

full structural relaxation. The results show that the incorporation of Cu in GaN leads to a net moment of 1 μ_B/Cu and p-like doping, consistent with earlier calculations[9-12]. Shown in Fig. 4 is the calculated local density of states (DOS) for substitutional Cu impurities in GaN. For simple substitution (Cu_{Ga}), the neighboring N atoms hybridize throughout the GaN bands, with the Cu states (from the top of the Ga-Cu bands) extending into the bulk gap. In non-spin-polarized calculations, the localization and partial occupation of these Cu gap states give rise to a Stoner-like magnetic instability, and thus substitutional Cu-doping in defect-free GaN should lead to a net local magnetization, which might order ferromagnetically. (Since only ferromagnetic ordering between the 72 atom supercells was considered, other orderings of the local Cu moments are not ruled out. In addition, the ordering energies at these concentrations are much smaller than the energies for the formation of the local moments, we have focused on the local electronic and magnetic properties.)

Earlier calculations have shown that intrinsic defects such as N vacancies can play a critical role in the magnetic properties of Cu-doped GaN[12]. However, in our previous studies of Mn-doped GaN grown by N_2/H_2 plasma, defects such as Ga vacancies and Mn interstitials were found not to contribute significantly to the magnetism, while only the N split interstitial neighboring a substitutional Mn configuration produces a Ga polarization observed in x-ray magnetic circular dichroism studies[28]. Although the N split interstitial is shown to be the ground state configuration for N interstitial in GaN, its formation energy is more than 3 eV[27], and therefore unlikely to form under equilibrium growth conditions. Nevertheless, the addition of hydrogen changes the growth conditions from Ga-rich to N-rich, and therefore could promote the formation of N split interstitials in our experiments. Hence, we consider the effect of an N split-interstitial defect neighboring the magnetically active substitutional Cu_{Ga} (Fig. 4 inset). Shown in

Fig. 4(b) is the local DOS at the Cu site (where the Cu is effectively 5-fold coordinated) that consists of the (filled) Cu d-states within the GaN bands, and states above and below the bulk bands that are primarily related to the N split-interstitial. In particular, the states around E_F are strongly related to the N split-interstitial, with relatively little weight on the Cu. (Fixed moment GGA+U calculations, with U-J=2-6 eV, similarly find this defect configuration suppresses the magnetic moment.) Furthermore, our calculations show an extremely strong attraction between Cu and N split-interstitial defects (~4 eV/Cu-N defect, relative to separated substitutional Cu and N split-interstitial defects), providing a large driving force for the formation of this configuration, and the suppression of the magnetic moment by this intrinsic defect.

This suppression of magnetic moments in Cu-doped GaN is in sharp contrast to the cases of GaN and ZnO doped with magnetic elements. For example, for Mn-doped GaN, the configuration of Mn_{Ga} neighboring an N split interstitial induces a Ga moment that is antiparallel to that of the Mn[28]. In the case of Co-doped ZnO, our calculations show that the large local moments of 3 μ_B per substitutional Co is preserved in the presence of intrinsic defects such as vacancies, and even increases to ~3.5 μ_B for the case of Zn vacancies.

In Fig. 5 we show the calculated x-ray absorption (XAS) and x-ray magnetic circular dichroism (XMCD) spectra for substitutional Cu, including the effects of the core hole. (The corresponding spectra without the core-holes are given in the inset.) For Cu near a N split-interstitial, there is no XMCD signal since there is no moment; for the simple substitution case, the XMCD and XAS are approximately the same since the states above E_F [cf., Fig. 4(a)] are mainly of minority character. Clearly, the XAS (XMCD) for the substitutional Cu near N split-interstitial are shifted by ~1.5 eV to higher energy compared to the simple Cu_{Ga}. (Note that the core hole affects the line shape of the defect complex significantly, whereas for the simple

substitution are similar with and without the core hole.) Previous XAS and XMCD experiments[13] on Cu-doped GaN wires showed two XAS peaks separated by 3.5 eV, with only the lower energy one (i. e., simple substitutional Cu) exhibiting a XMCD signal, consistent with the calculated spectra shown in Fig. 5[31].

IV. Conclusions

In summary, we have grown Cu-doped GaN thin films using MBE, and found that films grown with nitrogen plasma consist of two phases of CaCuN and Cu-rich alloys, while the addition of hydrogen into the nitrogen plasma leads to the suppression of the phase segregation and produces single-phased $Ga_{1-x}Cu_xN$ films with x as high as 0.04. However, these homogeneous $Ga_{1-x}Cu_xN$ films are found to be not ferromagnetic. These observations are explained by first principles calculations, which reveal that the presence of intrinsic defects such as N split-interstitials can significantly affect the electronic and magnetic properties of Cu-doped GaN. Other effects such as the dopant charge states and co-doping, which have shown to be important to the magnetism of Mn- and Fe-doped GaN[32,33], may also play a role in Cu-doped GaN. In addition, since p-type doping in GaN can also be compensated by hydrogen-dopant complexes[34-36], hydrogen related defects can also contribute to the suppression of ferromagnetic ordering in these films grown with N_2/H_2 plasma. These effects must be explored if the potential of Cu-doped GaN as a homogenous diluted magnetic semiconductor is to become a reality.

Acknowledgements

Financial support for this work is provided by the NSF (DMR-0706359). A portion of this research was conducted at the Center for Nanophase Materials Sciences, which is sponsored at

Oak Ridge National Laboratory by the Office of Basic Energy Sciences, U.S. Department of Energy.

References:

[1]H. Ohno, Science **281**, 951 (1998).

[2]T. Dietl et al., Science **287**, 1019 (2000).

[3]S. J. Pearton et al., J. Appl. Phys. **93**, 1 (2003).

[4]I. Žutić, J. Fabian, and S. Das Sarma, Rev. Mod. Phys. **76**, 323 (2004).

[5]C. Liu, F. Yun, and H. Morkoc, J. Mater. Sci.: Mater. Electron. **16**, 555 (2005).

[6]A. H. Macdonald, P. Schiffer, and N. Samarth, Nature Mater. **4**, 195 (2005).

[7]S. Kuroda, N. Nishizawa, K. Takita, M. Mitome, Y. Bando, K. Osuch, and T. Dietl, Nature Mater. **6**, 440 (2007).

[8]T. Dietl, Nature Mater. **9**, 965 (2010).

[9]R. Q. Wu, G. W. Peng, L. Liu, Y. P. Feng, Z. G. Huang, and Q. Y. Wu, Appl. Phys. Lett. **89**, 062505 (2006).

[10]A. L. Rosa and R. Ahuja, Appl. Phys. Lett. **91**, 232109 (2007).

[11]H. J. Xiang and S. –H. Wei, Nano Lett. **8**, 1825 (2008).

[12]B. Xu and B. C. Pan, J. Appl. Phys. **105**, 103710 (2009).

[13]H. –K. Seong, J. –Y. Kim, J. –J. Kim, S. –C. Lee, S. –R. Kim, U. Kim, T. –E. Park, and H. –J. Choi, Nano Lett. **7**, 3366 (2007).

[14]X. H. Ji, S. P. Lau, S. F. Yu, H. Y. Yang, T. S. Herng, and J. S. Chen, Nanotechnology **18**, 105601 (2007).

[15]L. Sun, F. Yan, H. Zhang, J. Wang, Y. Zeng, G. Wang, and J. Li, J. Appl. Phys. **106**, 113921 (2009).

[16]X. L. Yang, Z. T. Chen, C. D. Wang, Y. Zhang, X. D. Pei, Z. J. Yang, G. Y. Zhang, Z. B. Ding, K. Wang, and S. D. Yao, J. Appl. Phys. **105**, 053910 (2009).

[17]C. H. Choi, S. H. Kim, H. J. Lee, Y. H. Jeong, and M. H. Jung, J. Mater. Res. **24**, 1716 (2009).

[18]P. R. Ganz, G. Fischer, C. Sürgers, and D. M. Schaadt, J. Cryst. Growth **323**, 355 (2011).

[19]T. -H. Huang, P. R. Ganz, L. Changa, and D. M. Schaadt, J. Electrochem. Soc. **158**, H860 (2011).

[20]G. F. Sun, Y. Liu, Y. Qi, J. F. Jia, Q. -K. Xue, M. Weinert, and L. Li, Nanotechnology **21**, 435401 (2010).

[21]Y. Cui and L. Li, Appl. Phys. Lett. **80**, 4139 (2002).

[22]V. K. Lazarov, S. H. Cheung, Y. Cui, L. Li, and M. Gajdardziska-Josifovska, Appl. Phys. Lett. **92**, 101914 (2008).

[23]J. Neugebauer et al., Phys. Rev. Lett. **90**, 056101 (2003).

[24]S. T. King, M. Weinert, and L. Li, Phys. Rev. Lett. **98**, 206106 (2007).

[25]R. C. O'Handley, *Modern magnetic materials: principles and applications* (Wiley, 2000).

[26]A. Sundaresan and C. N. R. Rao, Nano Today **4**, 96 (2009).

[27]S. Limpijumnong and C. G. Van de Walle, Phys. Rev. B **69**, 035207 (2004).

[28]D. J. Keavney, S. H. Cheung, S. T. King, M. Weinert, and L. Li, Phys. Rev. Lett. **95**, 257201 (2005).

[29]A. Soudi, E. H. Khan, J. T. Dickinson, and Y. Gu, Nano Lett. **9**, 1844 (2009).

[30]M. Weinert, G. Schneider, R. Podloucky, and J. Redinger, J. Phys. Condens. Matter **21**, 084201 (2009).

[31]Our preliminary XAS studies shows only L_3 and L_2 peaks at 935 and 955 eV, respectively, suggesting that the Cu incorporated in our samples is likely associated with N split-interstitials. In the case of Cu-doped GaN nanowires [Ref. 13], the L_3 and L_2 are observed at 931 and 951 eV,

respectively, with additional peaks at 935 eV and 955 eV, which were attributed to trivalent state of Cu.

[32]A. Bonanni et al., Phys. Rev. B **84**, 035206 (2011).

[33]A. Navarro-Quezada et al., Phys. Rev. B **84**, 155321 (2011).

[34]S. Nakamura, N. Iwasa, M. Senoh, T. Mukai, Jpn. J. Appl. Phys., **31**, 1258 (1992).

[35]J. Neugebauer and C. G. Van de Walle, Phys. Rev. Lett. **75**, 4452 (1995).

[36]W. Gotz, N. M. Johnson, D. P. Bour, M. D. McCluskey, and, E. E. Haller, Appl. Phys. Lett. **69**, 3725 (1996).

Figure captions:

Fig. 1 Scanning electron microscopy images of $Ga_{1-x}Cu_xN$ films grown with (a) N_2 plasma, and (b) N_2/H_2 plasma. (c) EDS spectra taken at regions "A", "B", and "C" as marked in (a) and (b).

Fig. 2 X-ray diffraction patterns for a $Ga_{0.96}Cu_{0.04}N$ film 100 nm thick N_2/H_2 plasma. Inset: close-up view of the peaks around the GaN (0002) peak at 34.61°.

Fig. 3 Comparison of the magnetizations for $Ga_{1-x}N_x$/SiC films grown using N_2/H_2 plasma without (x=0) and with Cu doping (x=0.04). (a) Magnetic field dependence of the magnetization measured at 4.2 and 298 K. (b) Temperature-dependent of the magnetization with a 500 Oe field applied parallel to the surface of the films. All curves are normalized by the mass of the samples.

Fig. 4 Cu local density of states for (a) simple Cu_{Ga} (majority and minority) and (b) Cu_{Ga} next to a N split-interstitial (majority and minority the same). The shaded regions represent the calculated bulk GaN DOS, and the local structure of the N split-interstitial is given as the inset to (b).

Fig. 5 Calculated XAS and XMCD Cu L_{III} spectra for the simple Cu_{Ga} and next to a N split-interstitial. The effect of the core hole was included in the calculations, and the energy position was fixed from the differences in total energies of the systems with and without core holes. (The corresponding calculated $p_{3/2}$ energy in bulk metallic Cu is 931.4 eV compared to the experimental value of 932.5 eV.) The corresponding XAS (solid line) and XMCD (dashed line)

spectra for calculations ignoring the core hole (with the energies set by the initial state core eigenvalues) are given in the inset.

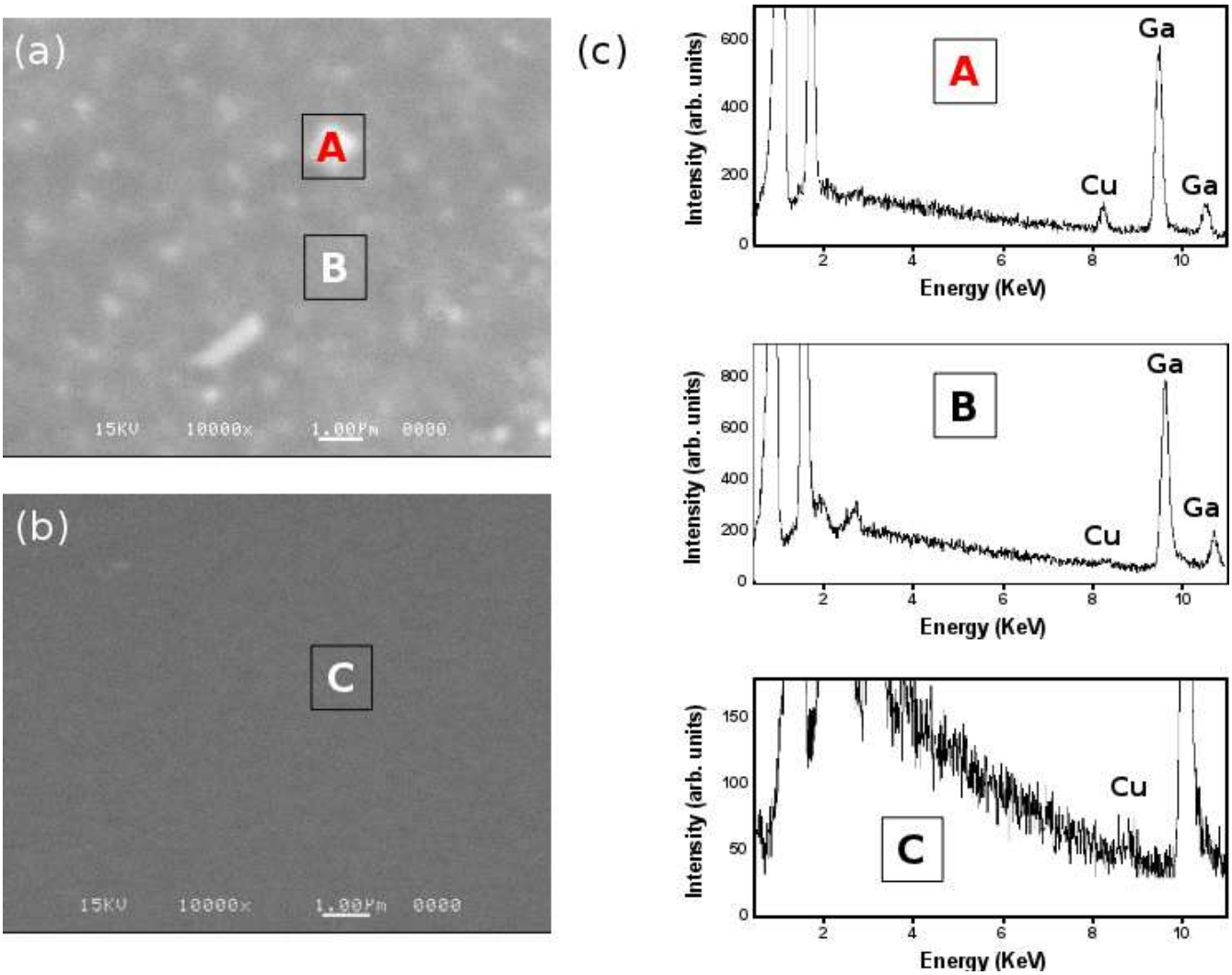

Figure 1 BK11628 27JAN2012

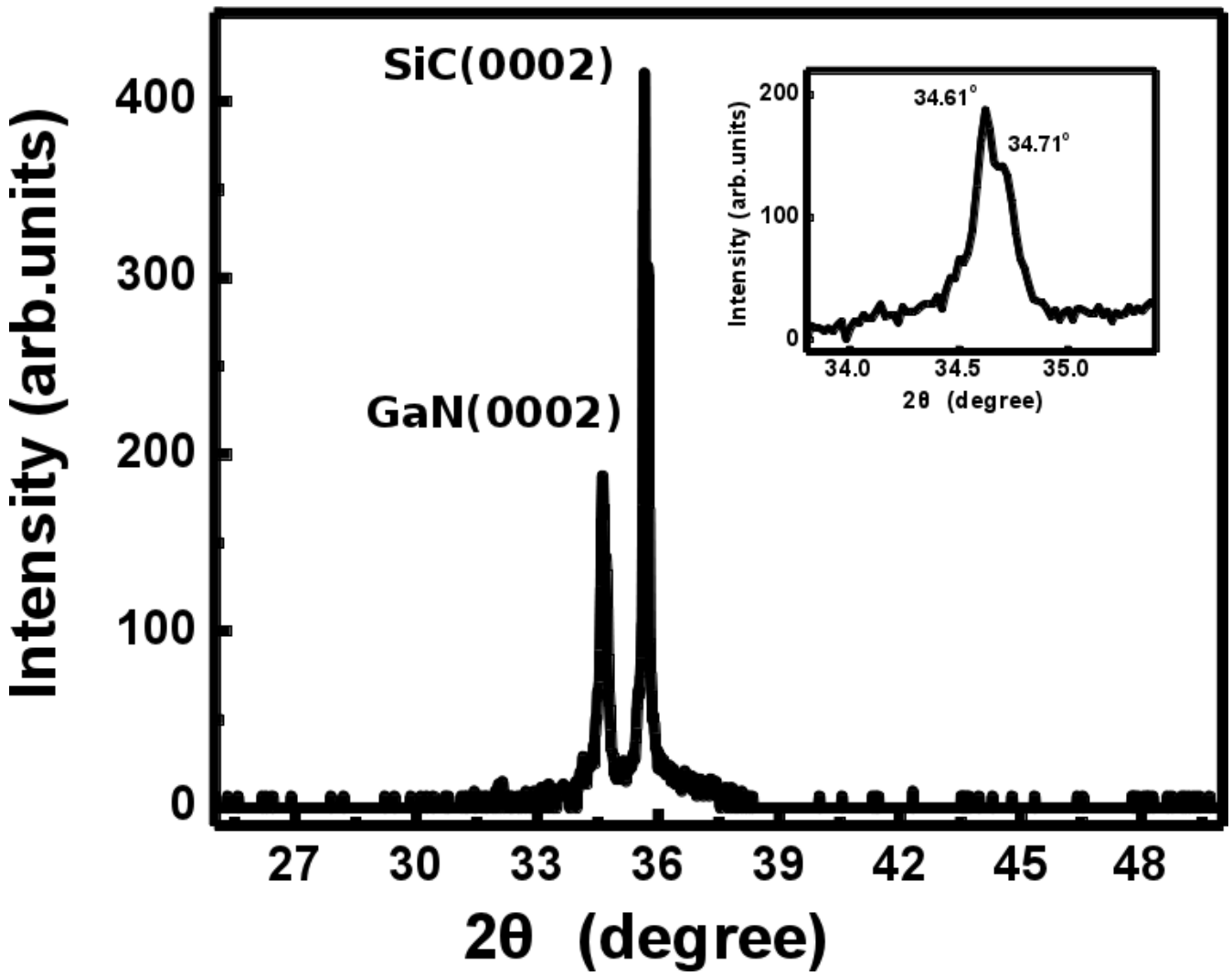

Figure 2 BK11628 27JAN2012

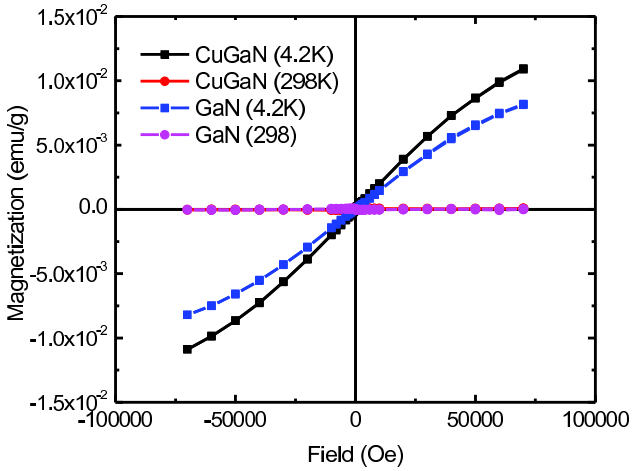

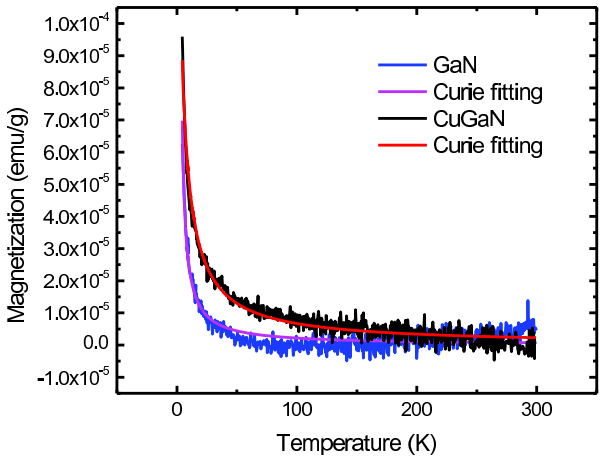

Figure 3 BK11628 27JAN2012

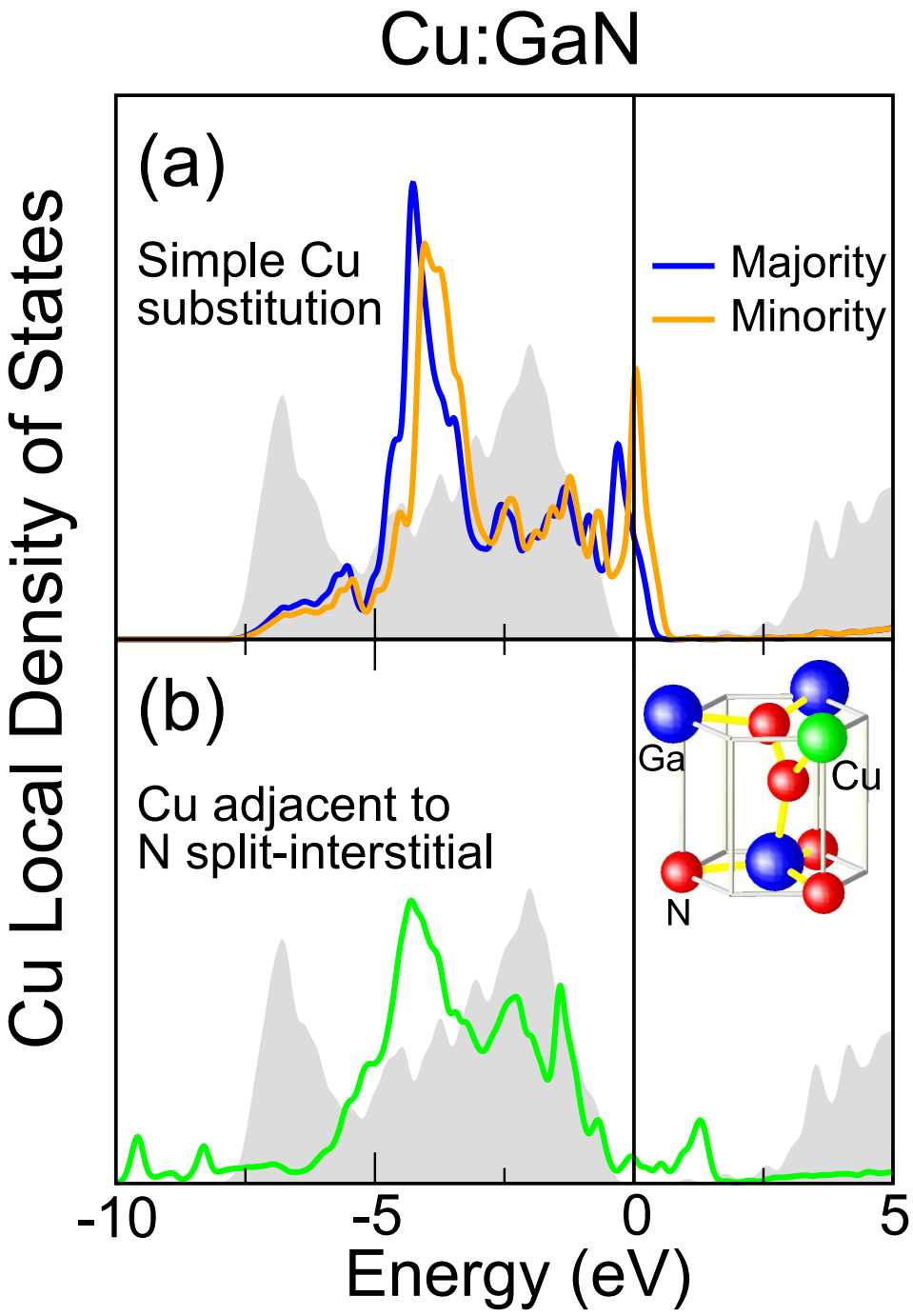

Figure 4 BK11628 27JAN2012

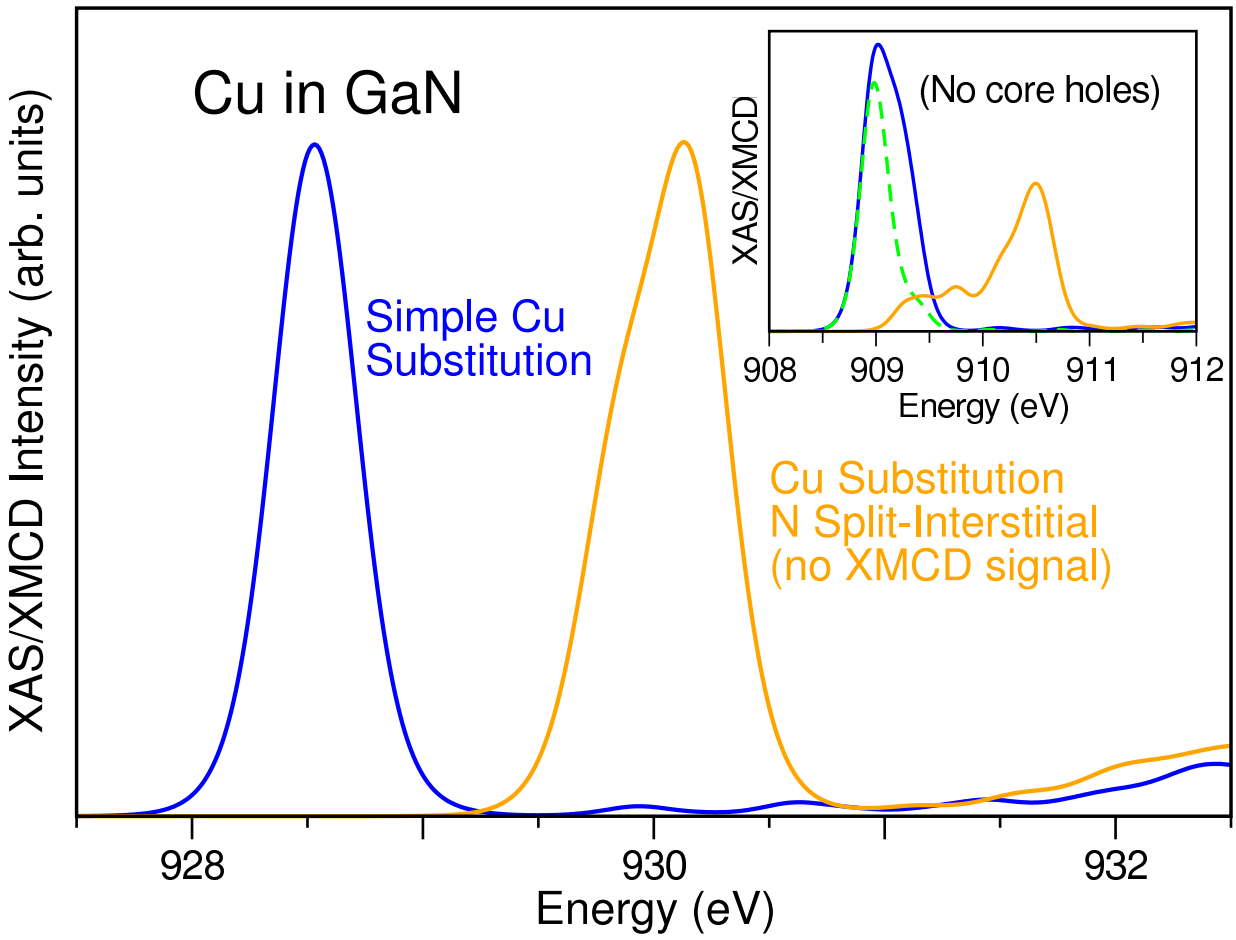

Figure 5 BK11628 27JAN2012